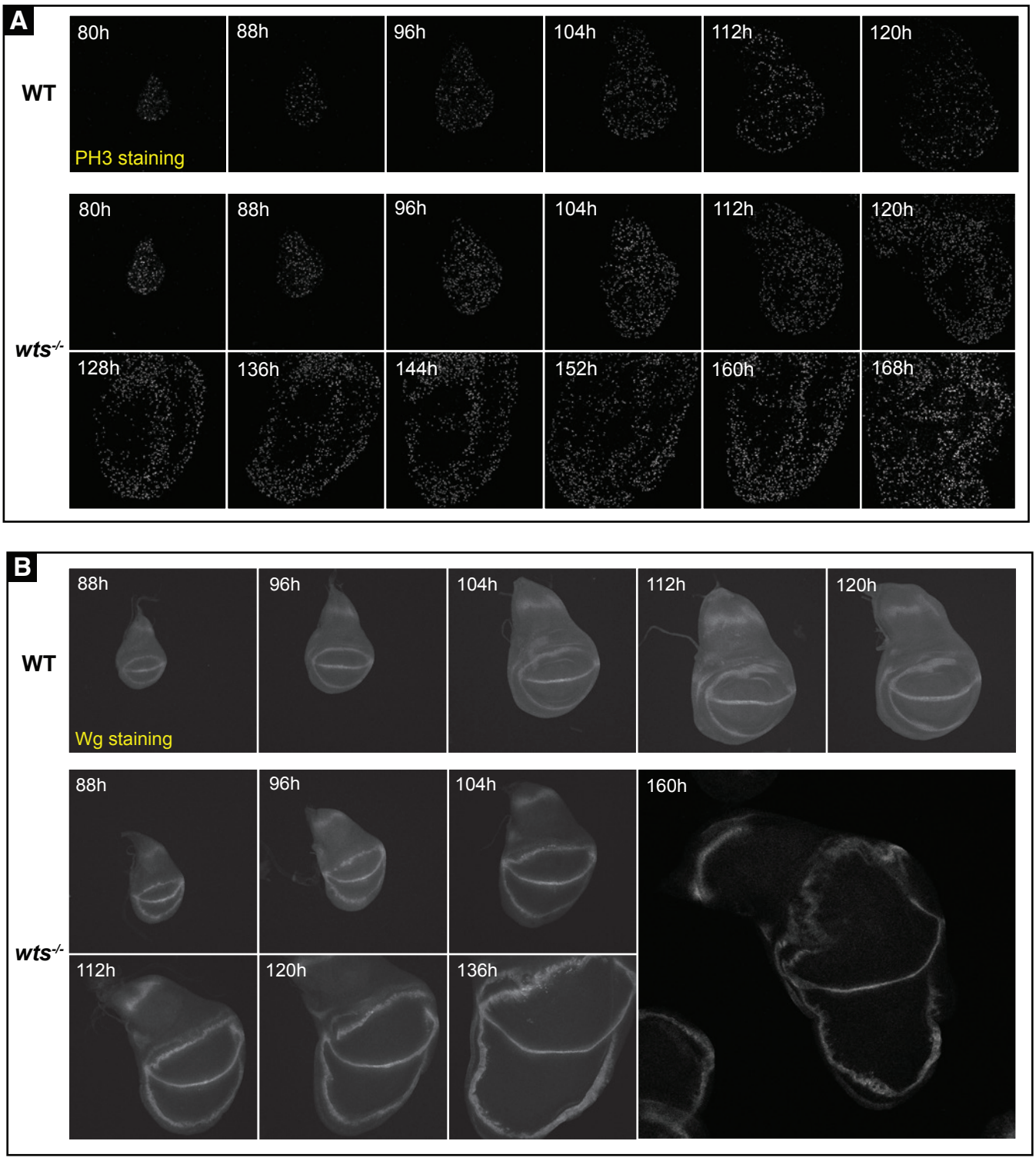

Figure 1: Proliferation and growth anisotropy phenotype of the *wts*$^{P2/P2}$ (*wts*$^{-/-}$) hypomorph mutant compared to wild-type (WT).

(A) Phospho-histone H3 staining (PH3), which positively marks cells in mitosis, in WT control discs and in *wts* mutant discs of the same age. All images are at the same scale. WT discs display an homogeneous repartition of dividing cells, unlike *wts* mutant discs. However, discs of the same age appear of similar sizes.

(B) Wingless (Wg) staining of WT and *wts* mutant discs of the same age. Wg marks the edge of the wing pouch as well as the dorso-ventral boundary. All images are at the same scale.

In all images, age is given in hours after egg laying.

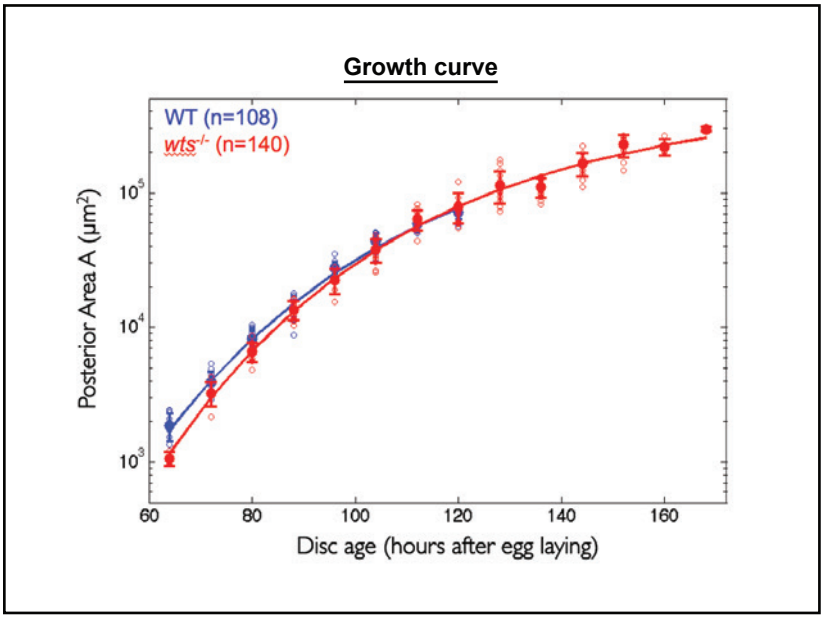

Figure 2: Growth curve of WT and *wts* mutant wing discs.

Graph representing the size of the wing posterior area in function of disc age.
wts mutant discs do not appear bigger than WT discs during the normal growth period (until 120 hours after egg laying). However, *wts* mutant larvae do not pupariate at 120 hours after egg laying and *wts* discs keep on growing for several days afterwards.

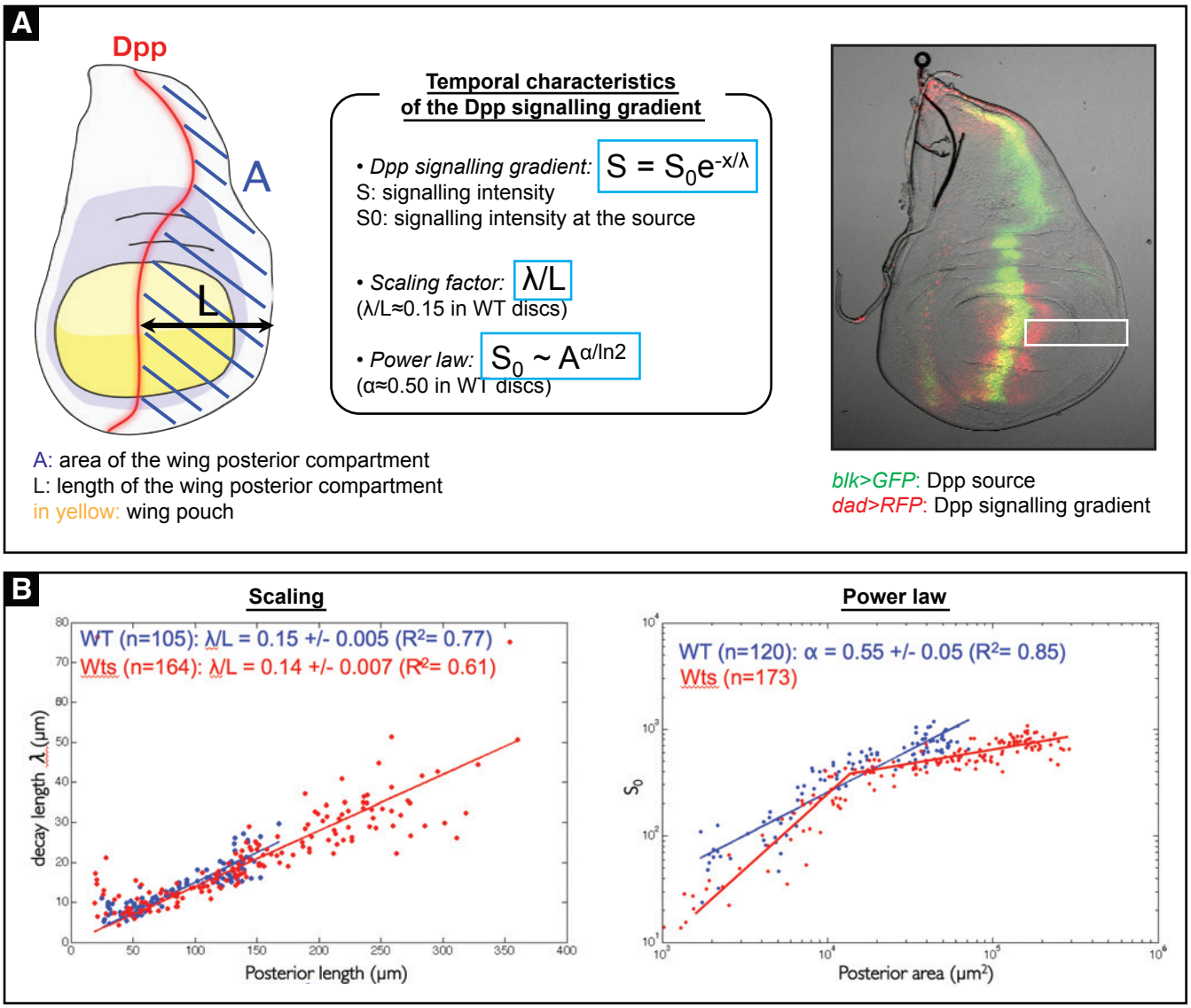

Figure 3: *wts* mutant wing discs present a modification of some but not all temporal characteristics of the Dpp signalling gradient.

(A) Presentation of the temporal characteristics of the Dpp gradient in WT discs (from Wartlick et al, Science, 2011). The image on the right is a superposition of the brightfield image of a third instar wing disc and of two fluorescent images showing the expression of GFP under the *blk* promoter (in green) and of RPF under the *dad* promoter (in red). The white rectangle represents the zone where the Dpp signalling gradient is measured (dorsal posterior compartment).
(B) Depiction of the measurements that allow to apprehend the scaling factor and power law relationship in WT and *wts* mutant discs. On the left, graph representing the decay length of the Dpp signalling gradient in function of the posterior length of the same disc. Scaling is not affected in *wts* mutant discs. On the right, graph representing the Dpp signalling intensity at the source in function of the posterior area. The power law is affected in *wts* mutant discs and displays a two-phase behaviour.

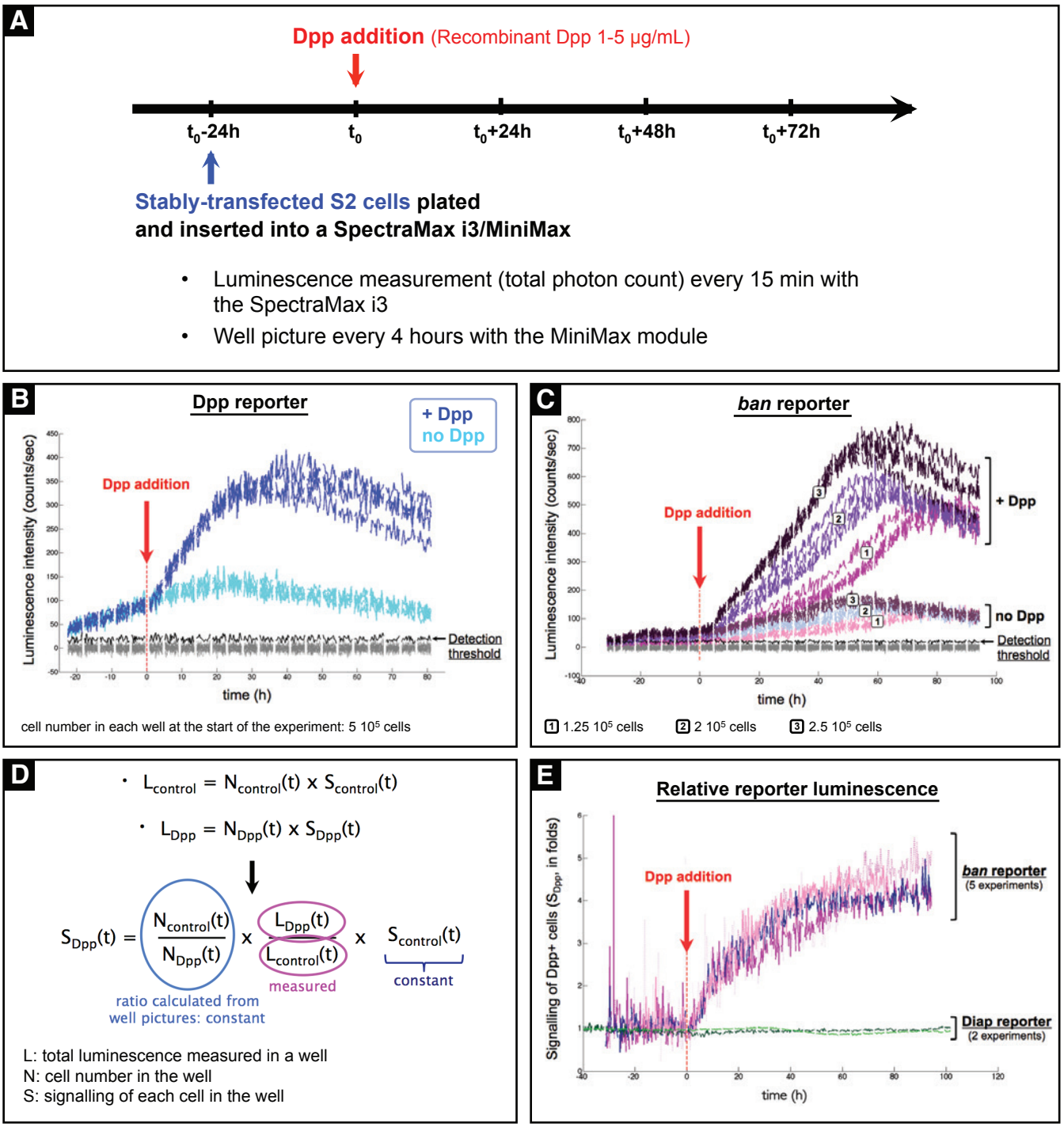

Figure 4: Study of the adaptation of the Hpo pathway in response to Dpp addition in S2 cells.
(A) Experimental set-up to measure the temporal response of various luminescent reporters in stably-transfected S2 cell lines.
(B) Temporal behaviour of the stably-transfected Dpp reporter line after addition of recombinant Dpp to the wells. The reporter responds: the added recombinant Dpp is functional in our system.
(C) Temporal behaviour of one of the stably-transfected *ban* reporter lines after addition of recombinant Dpp. The total response of the wells depends on cell concentration (three different cell concentrations are shown).
In (B) and (C), four replicates for each condition are shown. The grey curves are control curves that are used to measure the background and to calculate the detection threshold (black line).
(D) Methodoligical scheme to extract single cell luminescence responses from total well luminescence.
(E) Temporal behaviour of the *ban* and Diap reporters after normalisation (explained in D). Five experiments (with three different cell concentrations) are shown for the *ban* reporter, and two for the Diap reporter. All *ban* reporter curves collapse and show a 4-fold exponential increase after Dpp addition. The Diap reporter is insensitive to Dpp addition.